

## OPEN

# Topical Application of Mesenchymal Stromal Cells Ameliorated Liver Parenchyma Damage After Ischemia-Reperfusion Injury in an Animal Model

Ping Kuen Lam, PhD,<sup>1,2</sup> Charing Ching Ning Chong, FRCS,<sup>1,2</sup> Anthony Wing Ip Lo, FHKCPath,<sup>3</sup> Anthony Wing Hung Chan, FRCPA,<sup>3</sup> Cindy See Wai Tong, MSc,<sup>1,2</sup> Don Wai Ching Chin, BSc,<sup>1,2</sup> Kenneth Hoi Kin Wong, MPhil,<sup>4</sup> Richard Kwong Wai Choy, PhD,<sup>4</sup> Andrew Kai-Yip Fung, FRCS,<sup>1</sup> Yi Xiang Wang, MD,<sup>5</sup> Ka Fai To, MD,<sup>3</sup> Paul Bo San Lai, MD<sup>1,2</sup>

**Background.** Ischemia-reperfusion injury (IRI) is commonly encountered after liver surgery. This study evaluated the hepatoprotective effects of topically applied adipose-derived mesenchymal stromal cells (ADMSCs) on hepatic IRI in a rat model. **Methods.** ADMSCs from transgenic green fluorescent protein Sprague-Dawley rats were topically applied to the liver surface of Sprague-Dawley rats after hepatic IRI and fixed in position by fibrin glue (group A, n = 24). An equivalent amount of ADMSCs were administered through the portal (group B, n = 24) or tail vein (group C, n = 24). In the control group (group D, n = 20), no treatment was given to the IRI liver. **Results.** All the rats in group A and group D survived. Within 2 days after hepatic IRI, only 50% of rats survived in group B, and ADMSCs were detected in thromboemboli within large vessels. 62.5% of the rats died in group C because most of the ADMSCs were trapped in the lungs. ADMSCs migrated across the liver capsule and homed to the injured liver parenchyma 3 days after topical application in group A. The homed ADMSCs expressed hepatocyte nuclear factor-4 $\alpha$  and hepatocyte nuclear factor-1. Compared with group D, the rate of hepatic regeneration in group A was enhanced with less inflammation, smaller necrotic areas, and improved liver function. Proinflammatory cytokines IL-6, IL-21, and CD70 were significantly downregulated in group A by 6.3-, 2.7-, and 12.7-fold, respectively ( $P < 0.05$ ). The neurogenic locus NOTCH homolog protein pathway was activated in the topical ADMSCs. **Conclusions.** Topically applied adipose-derived mesenchymal stromal cells demonstrated hepatoprotective effects on hepatic IRI in an animal model.

(*Transplantation Direct* 2017;3: e160; doi: 10.1097/TXD.0000000000000675. Published online 11 May, 2017.)

**T**ransient hepatic inflow occlusion (Pringle maneuver) is a technique that can reduce intraoperative blood loss during liver resection. However, interruption of hepatic inflow causes degradation of mitochondrial adenosine triphosphate and alters biochemical homeostasis.<sup>1</sup> Additionally, reperfusion

induces further liver damage by activating Kupffer cells, neutrophils and the innate immune system.<sup>2</sup> Hepatocellular damage and dysfunction are the consequences of ischemia-reperfusion injury (IRI).

Received 21 February 2017.

Accepted 7 March 2017.

<sup>1</sup> Department of Surgery, The Chinese University of Hong Kong, Prince of Wales Hospital, Shatin, Hong Kong.

<sup>2</sup> Chow Tai Fook-Cheng Yu Tung Surgical Stem Cell Research Centre, The Chinese University of Hong Kong, Prince of Wales Hospital, Shatin, Hong Kong.

<sup>3</sup> Department of Anatomical and Cellular Pathology, The Chinese University of Hong Kong, Prince of Wales Hospital, Shatin, Hong Kong.

<sup>4</sup> Department of Obstetrics and Gynaecology, The Chinese University of Hong Kong, Prince of Wales Hospital, Shatin, Hong Kong.

<sup>5</sup> Department of Imaging and Interventional Radiology, The Chinese University of Hong Kong, Prince of Wales Hospital, Shatin, Hong Kong.

The authors declare no funding or conflicts of interest.

P.K.L., C.C.N.C. contributed equally and are the co-first authors. P.K.L., C.C.N.C., A.W.I.L., A.K.Y.F. and P.B.S.L. designed the study, interpreted the results and wrote the manuscript. P.K.L. and P.B.S.L. supervised laboratory work and animal

experiments, respectively. A.W.I.L. and A.W.H.C. carried out histological examinations. C.S.W.T., K.H.K.W., R.W.K.C., Y.X.W. performed laboratory work. D.W.C.H. conducted animal experiments.

Correspondence: Prof Paul BS Lai, Department of Surgery, The Chinese University of Hong Kong, Prince of Wales Hospital, Shatin, Hong Kong. (paullai@surgery.cuhk.edu.hk).

Supplemental digital content (SDC) is available for this article. Direct URL citations appear in the printed text, and links to the digital files are provided in the HTML text of this article on the journal's Web site ([www.transplantationdirect.com](http://www.transplantationdirect.com)).

Copyright © 2017 The Author(s). *Transplantation Direct*. Published by Wolters Kluwer Health, Inc. This is an open-access article distributed under the terms of the Creative Commons Attribution-Non Commercial-No Derivatives License 4.0 (CCBY-NC-ND), where it is permissible to download and share the work provided it is properly cited. The work cannot be changed in any way or used commercially without permission from the journal.

ISSN: 2373-8731

DOI: 10.1097/TXD.0000000000000675

Mesenchymal stromal cells (MSCs) can be induced to differentiate into ectodermal and endoderm lineages under specific conditions.<sup>3</sup> Published studies have shown the effects of MSCs in chronic carbon tetrachloride-induced injury and IRI.<sup>4-7</sup> MSCs can be administered by systemic infusion but the infused MSCs can be trapped in the pulmonary capillaries.<sup>8</sup> Conversely, direct injection of MSCs to the liver is associated with bleeding, whereas infusion into the portal vein can cause portal hypertension.<sup>9</sup>

Our previous studies have shown that topical applied MSCs can migrate into the injured tissues.<sup>10,11</sup> In this study, the hepatoprotective effects after hepatic IRI and the potential underlying mechanisms were investigated.

## MATERIALS AND METHODS

All animal procedures were conducted in accordance with the guidelines of the Animals (Control of Experiments) Ordinance Chapter 340, Department of Health, Hong Kong, and with approval from the Animal Experimentation Ethics Committee of the Chinese University of Hong Kong.

### Adipose-Derived MSCs

Adipose-derived MSCs (ADMSCs) were harvested from the subcutaneous adipose tissue of male transgenic Sprague-Dawley rats (300-350 g) that expressed green fluorescent protein (GFP) (SD-Tg (CAG-EGFP) CZ-0040sb; SLC Inc, Japan). The adipose tissue was washed with sterile phosphate-buffered saline (PBS) and treated with 0.1%-collagenase (type I; Sigma-Aldrich) in PBS for 30 minutes at 37°C. After filtration through a 100- $\mu$ m mesh filter, the filtrate was washed three times and suspended in Dulbecco modified Eagle medium with 10% fetal bovine serum, 100 units/mL penicillin, 100  $\mu$ g/mL streptomycin, and 2 mM L-glutamine (Invitrogen, USA). The cultures were maintained in humidified atmosphere of 5% CO<sub>2</sub>.

### Cell Phenotyping

ADMSCs were grown for 3 to 5 passages, then harvested with 0.25% trypsin/ethylenediaminetetraacetic acid and characterized by flow cytometer with a FACScan argon laser (BD Bioscience, San Jose, CA). Trypsinized cells were washed and centrifuged for 10 minutes at low speed, and then  $1 \times 10^6$  cells were fixed in 3% paraformaldehyde for 30 minutes at 4°C. The cells were labeled with phycoerythrin-conjugated antibodies against CD29, CD45, and CD90 (Abcam Inc, Cambridge, UK). Isotype-matched negative controls were used to assess background fluorescence, and analyzed by Cell-Quest software (Becton Dickson).

### Adipogenic, Chondrogenic, and Osteogenic Differentiation Potential

ADMSCs were seeded at 5000 cells/cm<sup>2</sup> and cultured in adipogenic, chondrogenic, and osteogenic differentiation culture media (Invitrogen, Life Technologies, China). The differentiated adipocytes were stained with Oil-Red-O, chondrocytes with Alcian-Blue, and osteocytes with Alizarin-Red-S stain (Sigma-Aldrich, Inc) to identify intracytoplasmic lipid, extracellular glycosaminoglycans and calcium deposits, respectively.

### IRI and Cell Transplantation

Wild-type female Sprague-Dawley rats (300-400 g, University Laboratory Animal Service Centre) were anesthetized

by intraperitoneal injection of ketamine (125 mg/kg). After midline laparotomy, the liver was exposed, and the portal triad was dissected. Hepatic ischemia was induced by the application of a bulldog clamp for 90 minutes to the inflow arterial and portal venous blood supply to the median and left liver lobes.<sup>12</sup> Reperfusion was confirmed by restoration to normal color of the ischemic lobes within 3 to 4 minutes after the clamp removal. The control group underwent the same laparotomy procedures, except that the blood supply to the liver was not interrupted.

ADMSCs were used for transplantation at passages 3 to 5. The cells were washed twice in PBS and counted. ADMSCs were transplanted immediately after the hepatic IRI. Cell viability was greater than 90% on trypan blue dye exclusion. In group A (n = 24),  $4 \times 10^6$  ADMSCs suspended in 250- $\mu$ L PBS were applied directly to the surface of the ischemic liver lobes. Two hundred fifty microliters of fibrin glue (Tisseel, Baxter Healthcare S.A., Wallisellen, Switzerland) was applied to hold the ADMSCs onto the liver surface. An equivalent amount of ADMSCs was transplanted by local infusion via the portal vein (group B, n = 24) or systemic infusion via the tail vein (group C, n = 24) using a Hamilton syringe with a 26-gauge needle. In the control group, no treatment was given to the IRI liver (group D, n = 20). For the transcriptome analysis, an equivalent amount of ADMSCs and fibrin glue were topically applied onto the liver without IRI (group E, n = 3). Before the abdomen was closed, 1 mL of normal saline was administered as fluid replacement. All rats were housed in a temperature-controlled room with a 12-hour light/dark cycle and ad libitum access to food and water.

### Histology, Immunohistochemistry, and Biochemistry

On days 3 to 5, 7 to 10, and 14 to 16 after ADMSC transplantation, the rats were sacrificed by exsanguination under pentobarbital anesthesia, and the livers were examined. Blood was collected for determination of alanine transaminase. The weights of the rat livers were measured.

Paraffin sections of the IRI liver were examined histologically. Standard immunohistochemical stainings with rabbit anti-GFP (Abcam Inc., Cambridge, UK) and mouse rat-specific anti-Ki67 (Dako, Denmark) were performed to study the trafficking of topical ADMSCs and cellular proliferation, respectively.

### ADMSC Labeled With CM-Dil and Immunofluorescence Staining

MSCs derived from the adipose tissue of wild-type Sprague-Dawley (SD) rats were labeled with 5-g/mL red fluorescence dye CM-Dil (Molecular Probes, Life Technologies). Ten-micron frozen sections of liver containing CM-Dil labeled ADMSCs were fixed with ice-cold acetone and incubated with antihepatocyte nuclear factor (HNF)-1 (Santa Cruz Biotechnology, USA) or anti-HNFr-4 $\alpha$  (HNF-4 $\alpha$ ) (Santa Cruz Biotechnology, USA), with fluorescein isothiocyanate-labeled second antibody, and mounted with antifade reagent containing 4',6-diamidino-2-phenylindole, dihydrochloride (Molecular Probes, Life Technologies).

### In Vitro Magnetic Labeling of MSCs with Superparamagnetic Iron Oxide

4.5-g/mL superparamagnetic iron oxide (SPIO) was used for ADMSCs labeling for 16 hours at ambient temperature before transplantation. The labeling condition and procedures

were performed per our previous study.<sup>13</sup> Prussian blues staining on paraffin sections were used to detect SPIO.

### Reverse Transcription Polymerase Chain Reaction Array

The liver specimens were fixed in buffered formalin for 24 hours and embedded in paraffin blocks. Five-micron histological sections were stained with hematoxylin and eosin. The regenerative scars were identified from the paraffin sections and then micro-dissected with a 21G needle. Materials from 10 to 20 slides were pooled. Ribonucleic acid (RNA) was extracted from the paraffin sections, empirically amplified and underwent reverse transcription polymerase chain reaction (RT-PCR) using commercially available primer sets. The RNA levels of 84 common rat cytokine genes were studied using RT-PCR arrays (Qiagen).

### Microarray of Topical ADMSCs

Three days after topical application, ADMSCs and liver tissue were harvested from the surface of the liver in group A ( $n = 3$ ) and group E ( $n = 3$ ) and immediately snap-frozen in liquid nitrogen and stored at  $-80^{\circ}\text{C}$ . The extracted RNA were hybridized with Agilent 4x44K Rat Gene Expression Microarray.

The data were analyzed with GeneSpring GX12.5 (Agilent Technologies, Santa Clara, CA). The gene expressions of “ADMSC population on IRI liver” with twofold or higher change and  $P$  values of 0.05 or less were compared with “ADMSC population on normal liver” using the “ADMSC pellet” as reference. Pathways were predicted using Wikipathway databases pathway and Genespring12.5.

### Statistical Analyses

Statistical analyses were performed with  $\chi^2$  and Mann-Whitney  $U$  tests to compare qualitative and quantitative variables, respectively. Statistical significance was defined as a  $P$  value less than 0.05, and statistical calculations were performed on SPSS 21 software (IBM).

## RESULTS

### Adipose-Derived Mesenchymal Stem Cells Retained Multipotential Differentiation

Flow cytometry analysis showed the ADMSCs strongly expressed CD29 and CD90, but was negative for CD45 (Figure 1A). The ADMSCs isolated from the transgenic GFP-SD rats were adherent to the plastic culture flasks and exhibited spindle-shape morphology (Figure 1B). ADMSCs demonstrated in vitro potential to differentiate into adipocytes, chondroblasts, and osteoblasts under specific differentiating environments, resulting in the formation of lipid-filled cytoplasmic vacuoles (Figure 1C), chondroid-type extracellular matrix (Figure 1D), and calcified nodules (Figure 1E), respectively.

### Topical ADMSCs Alleviated Liver IRI

Interrupting both the portal venous and hepatic arterial blood supplies induced selective lobar ischemia in the rat model. IRI caused necrosis in liver parenchyma as early as 6 hours after the procedure. Massive necrosis of hepatocytes was observed. Regeneration around these necrotic areas consisted of fibroblastic stroma and prominent ductal proliferation on day 3. This was followed by marked expansion of

the fibroblast populations (Figures 2E, F) on day 6. At day 14, the liver showed only mild nodularity and focal capsular thickening signs as the remaining signs of ischemia-reperfusion (Figures 2A, B, C, D, E, F).

The IRI liver of group A had smaller ratios of necrotic area to regeneration scar compared with group D on day 3 and day 7 (Figure 2G). These scars consisted of spindle cells and proliferation of small ductules. Notably, in the presence of topical ADMSCs, there was only mild acute inflammation in the regeneration scar. Most of the ADMSCs were located distant from the necrotic foci and regeneration scar.

### Liver Function and Enhanced Liver Regeneration Were Improved by Topical ADMSCs

Compared with control (group D), the liver function of IRI liver in group A improved as early as day 1 after the topical application of ADMSCs. Markers of liver cell damage, such as serum alanine aminotransferase (ALT) level, were significantly lower in the group A by more than twofold ( $P < 0.01$ , Figure 3A). The initial surge of serum ALT in day 1 was a result of the significant acute hepatocyte damage in the untreated IRI livers. Topical application of MSCs limited this surge of ALT. These findings suggested that topical MSCs might ameliorate the hepatotoxic effects of IRI. Furthermore, there was enhanced regeneration of injured hepatocytes in the presence of topical MSCs.

Rats were sacrificed at different time points after IRI to study the changes in wet weights of the recovering livers. The injured livers increased at a rate of 0.43 g/d of wet weight in group A, compared with 0.20 g/d in group D. In group A, the wet weight overshoot above the final wet weight of the healed liver (Figure 3B). The IRI liver of group A had smaller ratios of necrotic area to regeneration scar compared to group D on days 3 and 7 (Figure 3C).

Proliferation index Ki67 was lower in both the spindle cell population of the regeneration scar as well as the adjacent hepatocytes, on day 3 and day 7, respectively ( $P < 0.01$ , Figures 3D, E).

### IRI Rats Survived Topical Application of ADMSCs Better Than Portal Vein Infusion and Systemic Infusion

All rats with IRI that underwent topical ADMSCs application (group A) or received no treatment (group D) survived until they were sacrificed. In contrast, 50% rats that had portal venous ADMSCs infusion (group B) and 62.5% rats that had systemic ADMSCs infusion (group C) died within 2 days. ADMSCs were detected in thromboemboli within the large vessels of the group B surviving rats (Figures 4A, B). Viable ADMSCs were found around necrotic hepatocytes on day 2 in group A (Figures 4C, D).

For the ADMSCs that were infused via the tail vein (group C), none were detected in the injured liver because they were trapped within the pulmonary vasculature (Figures 4E, F). There was diffused interstitial pneumonitis with expansion of the alveolar septa by chronic inflammatory cells. However, ADMSC proliferation was not detected in the lung parenchyma.

### Topical MSCs Homed to the Liver Parenchyma

In group A, the ADMSCs were initially detected on the liver surface as a fibroblast-like proliferation (Figures 5A, B). In the rats that were sacrificed on day 1 after topical application of MSCs, there was no homing of MSCs to the liver parenchyma. On day 3, ADMSCs were observed at the peripheries of the islands of necrotic hepatocytes (Figures 5 C, D). The ADMSCs

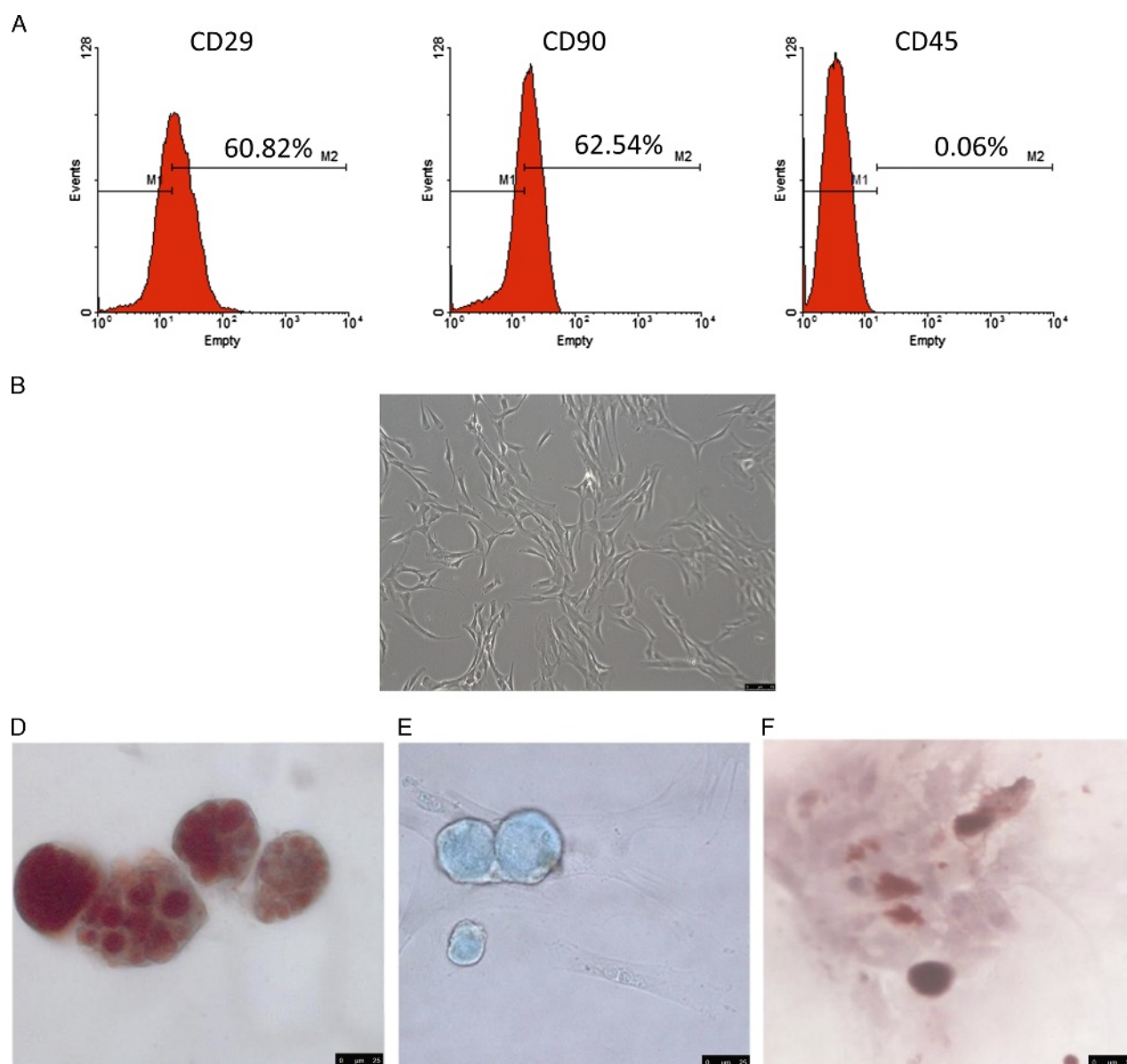


**FIGURE 1.** Flow cytometric analysis of ADMSCs using phycoerythrin-conjugated anti-CD29, anti-CD90 and anti-CD45 (A). ADMSCs in culture showed a spindle-shaped morphology (B), phase-contrast microscopy, ( $\times 200$ ). Under specific differentiating tissue culture conditions, these cells can form adipocytes with lipid-containing cytoplasmic vacuoles (C, Oil red O,  $\times 400$ ); chondrocytes with a rich glycosaminoglycan matrix (D, Alcian blue,  $\times 400$ ); and osteocytes with calcium-containing nodules (E, Alizarin Red S,  $\times 400$ ).

continued to proliferate and followed the innate liver regeneration framework, extending into the liver parenchyma (Figures 5E, F). ADMSCs were observed homing to the periphery of necrotic hepatocyte cell plates on day 10 (Figures 5G, H). No ADMSCs were detected in the IRI liver parenchyma on day 14 (Figures 5I, J). No GFP+ve cells were detected in other somatic organs. When fibrin glue was not added to fix the ADMSCs onto the surface of the injured liver (group D), most ADMSCs detached from the surface.

At all stages, ADMSCs exhibited spindle-shaped morphology. No GFP+ve cells were seen to develop the morphologies of differentiated cells, such as hepatocytes, epithelial cells of large ducts, or components of blood vessels, although they showed differentiation toward hepatic lineage. Using the pre-labeled red fluorescence dye, the ADMSCs coexpressed HNF-1 (Figure 5I) and HNF-4 (Figure 5J). However, these

markers were not expressed in ADMSCs that remained on the IRI liver surface (data not shown).

On day 3, SPIO nanoparticles were detected at the extracellular matrix at the periphery of the necrotic areas (Figures 5K, L). These iron particles were not transported to the necrotic areas by macrophages (Figure 5M). It was likely that the topically applied ADMSCs migrated through the liver capsule and homed to the necrotic areas. These ADMSCs died very quickly, probably due to the hostile environment of inflammation and necrosis, with subsequent release of the iron particles.

#### Proinflammatory Genes in Liver Parenchyma Were Suppressed

RT-PCR array demonstrated the downregulation of proinflammatory cytokines IL-6, IL-21, and CD70 in the IRI livers

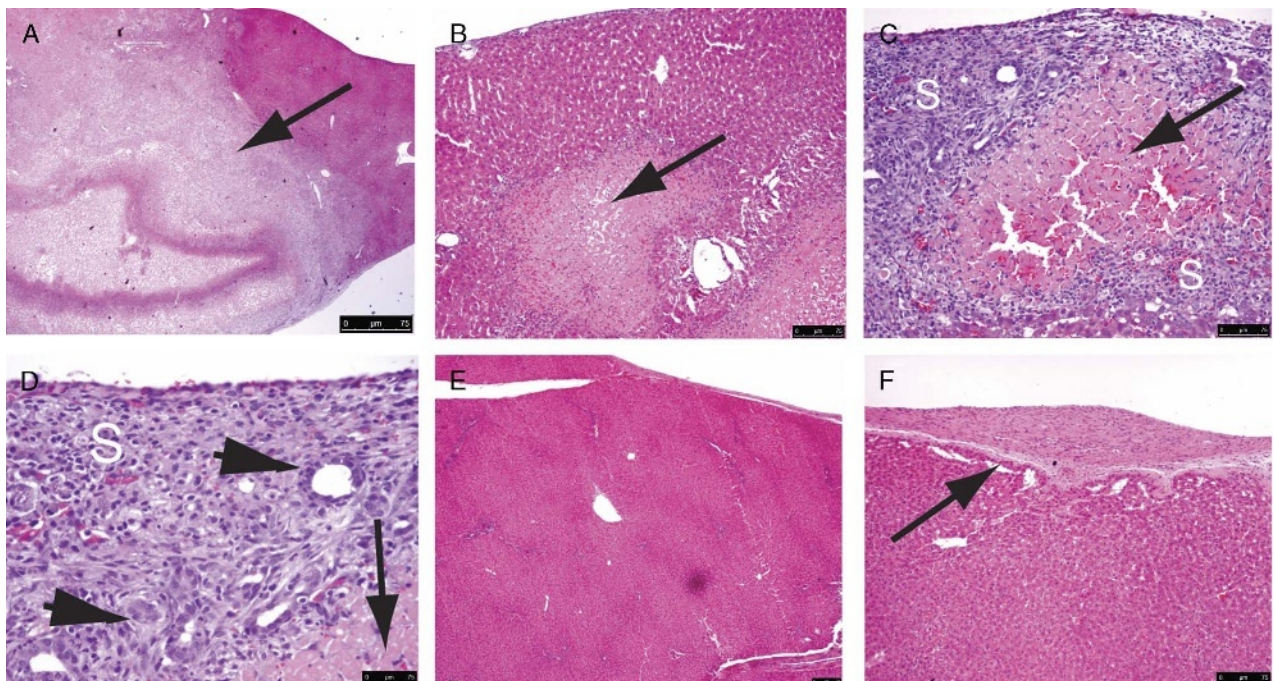


**FIGURE 2.** On day 3, posttransient occlusion of the hepatic vascular inflow, geographic necrosis (A to D, arrows, magnifications  $\times 40$ ,  $\times 100$ ,  $\times 200$ , and  $\times 400$ , respectively) was seen in the liver parenchyma, showing IRI. The surrounding regeneration scar (S) consisted of spindle cells and ductular proliferation (C and D, arrowheads). On day 14, the liver totally regenerated with resolution of the necrosis and regeneration scars, leaving minor nodularity of architecture (E,  $\times 100$ ), and minor thickening of the capsule (F, arrow,  $\times 200$ ).

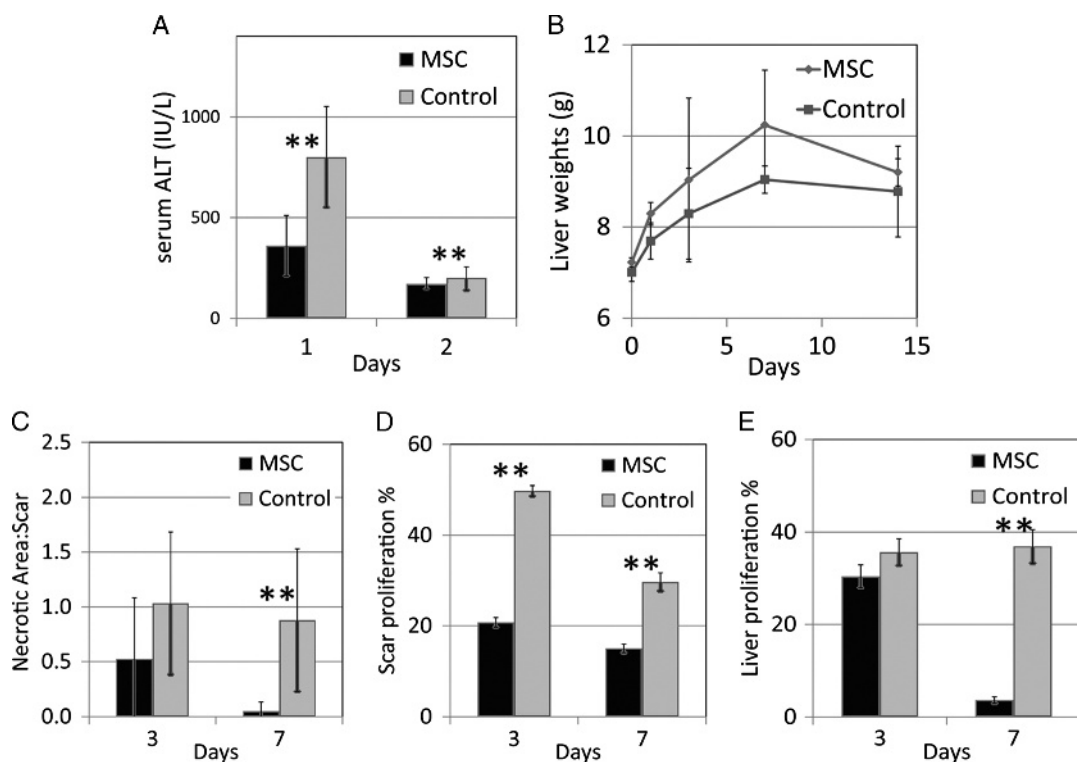


**FIGURE 3.** With application of topical stem cells, liver function recovered better, showing less surge of serum ALT (A  $**P < 0.01$ ) and higher rate of regeneration in terms of organ wet weight (B). The necrotic area to regeneration scar ratio was smaller in the IRI liver with topical stem cells (C,  $**P < 0.01$ ) on day 3 and day 7. The proliferation indices Ki67 in the spindle cells of the regeneration scar and the nearby hepatocytes were also lower in the IRI liver with topical stem cells (D and E, respectively).

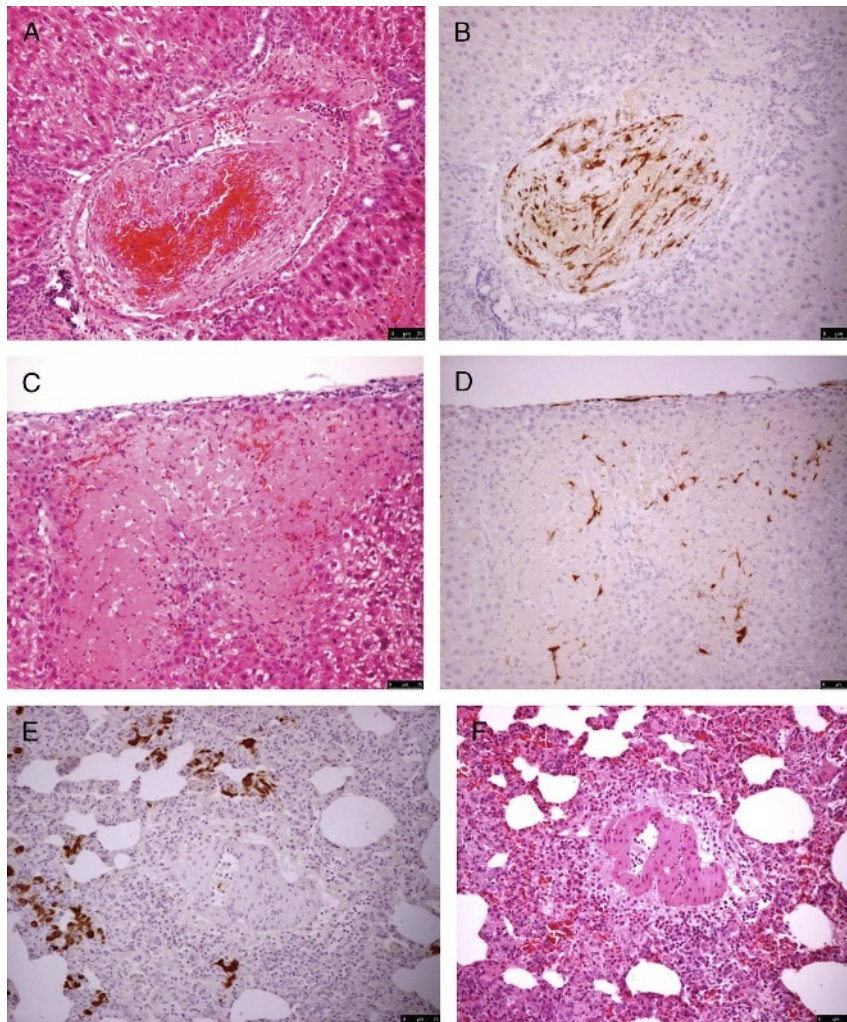


**FIGURE 4.** Local infusion of ADMSCs via the portal vein in the liver in Sprague-Dawley rats after IRI resulted in the formation of thromboemboli in large vessels (A and B, H&E and IHC, respectively,  $\times 400$ ). A small number of ADMSCs successfully homed to the periphery of foci of necrotic hepatocytes (C and D, H&E and IHC,  $\times 400$ , respectively). Systemic infusion of ADMSCs via the tail vein resulted in the trapping of exogenous stem cells in the lung (E, IHC  $\times 200$ ). Diffused interstitial pneumonia was observed (F, H&E  $\times 200$ ). H&E, hematoxylin and eosin; IHC, immunohistochemistry.

with topical ADMSCs by 6.3-, 2.7-, and 12.7-fold, respectively ( $P < 0.01$ ).

#### NOTCH Pathway Was Activated in Topical MSCs on the Surface of IRI Liver

To investigate the changes in gene expressions of the topical ADMSCs under the influence of the IRI liver microenvironment, transcriptomes of the MSCs on the liver surface on day 3 were studied. Hierarchical cluster analysis of the microarray data demonstrated 531 differentially expressed genes ( $P < 0.05$  and twofold upregulated or downregulated) between ADMSCs on the IRI liver surface and on the normal liver surface regarding the basal expression of the ADMSCs in vitro culture (Figure 6A). These genes covered a wide spectrum of genes related to liver metabolism (Figure 6B). Twenty genes were subsequently validated by RT-PCR (Table S1, SDC, <http://links.lww.com/TXD/A39>).

There were 21 pathways including the “NOTCH Pathway” that were significantly activated ( $P < 0.05$ ) in the topical ADMSCs on IRI liver (Table 1). The NOTCH Pathway is known to be important in regulating several fundamental cellular processes such as proliferation, apoptosis, migration

and differentiation. On day 3, the activation of NOTCH pathway-related genes in the topical ADMSCs on IRI liver was confirmed. Delta like-1 (DII-1), Notch 4,  $\gamma$ -secretase complex and Manic Fringe (Mfng) were also significantly upregulated, showing 23-, 1210-, 25-, and 217-fold changes, respectively. Other known pathways related to stem cell signaling, such as the Hedgehog Pathway and the Wnt Pathway, were not significantly changed in the topical applied ADMSCs.

#### DISCUSSION

In this study, partial hepatic ischemia was induced by interruption of the inflow blood supply to the median and left lobes in a rat model. The experimental rats could tolerate 90 minutes of partial hepatic ischemia as the outflow hepatic vein was not clamped. Hepatic IRI may cause up to 10% of early graft dysfunction after liver transplantation, leading to acute and chronic rejection.<sup>14,15</sup> Previous animal models have demonstrated that systemically or locally infused MSCs can migrate to sites of injury and facilitate tissue repair.

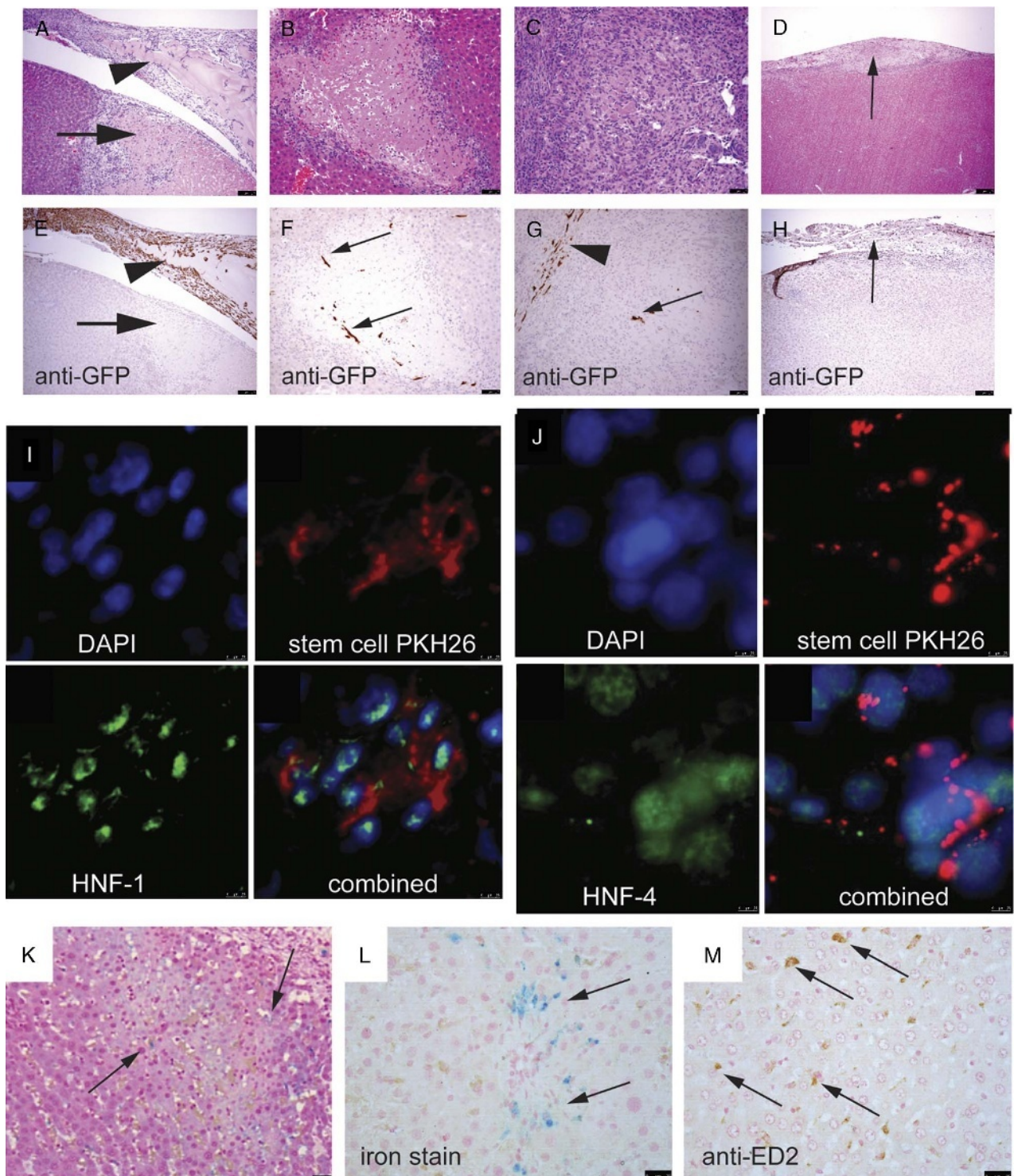


**FIGURE 5.** On day 3 postapplication of stem cells, most of the stem cells remained on the surface of the IR liver mixed with fibrin (A, arrowhead,  $\times 200$  and B showing immunohistochemical staining for anti-GFP). A necrotic area was seen immediately underneath the site of application (arrows). No stem cells were seen in this necrotic area. Small numbers of homed stem cells were seen at the periphery of the necrotic area (C and D,  $\times 200$ ). Some of the stem cells participated in the formation of the regeneration scar (E and F,  $\times 200$ ). At the end of day 14 but which regeneration was completed, no GFP+ve cells were detected in the thickened fibrous tissue (G and H, arrows) or the liver parenchyma. Homed stem cells expressed HNF-1 (I,  $\times 400$ ) and HNF-4 (J,  $\times 400$ ), showing differentiation toward hepatocyte lineage. When stem cells were fed with SPIO nanoparticles, these stem cells might have migrated to the periphery of necrotic area, but demised quickly, leaving the iron particles behind (K and L, arrows; H&E and iron stain,  $\times 200$ , respectively). These iron particles were not brought to the necrotic area by macrophages (M, arrows, immunohistochemical staining for anti-ED2).

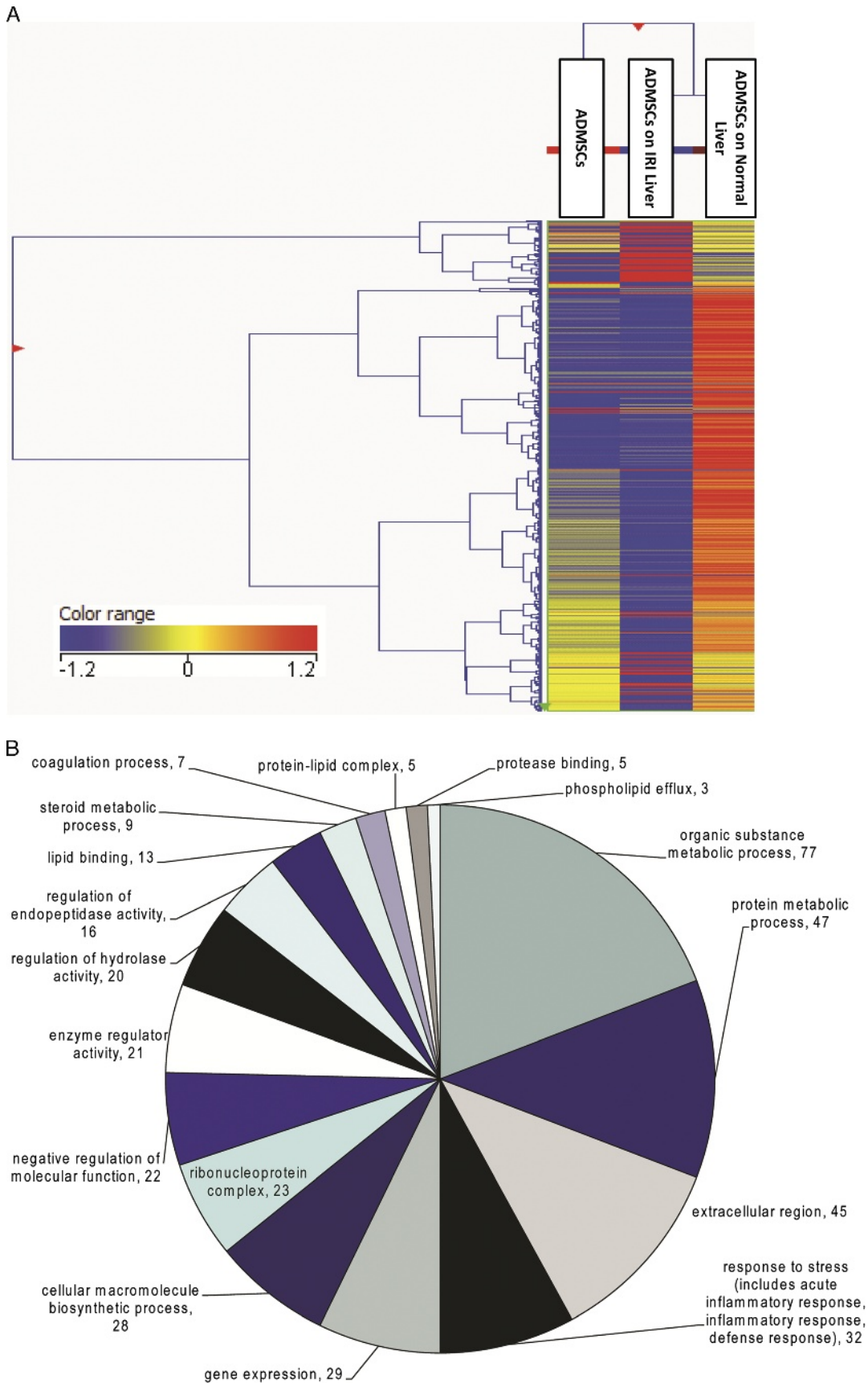


**FIGURE 6.** A, Heat map showed hierarchical cluster analysis of the differential expression of genes of naive ADMSCs in culture, topical ADMSCs on IRI liver and topical ADMSCs on normal liver. B, Pie chart demonstrated 531 genes covering a wide spectrum of genes related to liver metabolism.



**TABLE 1.****Ten activated pathways in the ADMSC population on the recipient surface of IRI liver and ranked per *P* values**

Pathways	<i>P</i>	Matched entities	Pathway entities	Mean absolute fold change
Activation of matrix metalloproteinases	0.029	3	12	56.1
Notch signaling pathway WP517_41730	0.036	6	44	53.1
PPARA activated gene expression	0.023	2	5	45.1
ACE inhibitor pathway WP557_41786	0.012	3	8	36.6
Recycling of bile acids and salts	0.001	4	8	25.6
Synthesis and degradation of ketone bodies WP349_48271	0.036	2	5	20.0
FAS pathway and stress induction of HSP regulation WP89_47779	0.007	7	37	12.6
IL-6 signaling	0.036	2	5	9.7
Synthesis of bile acids and bile salts via 7 $\alpha$ -hydroxycholesterol	0.012	3	10	9.1
Scavenging of heme from plasma	0.023	2	4	6.7

PPARA, Peroxisome Proliferator Activated Receptor Alpha; ACE, Angiotensin Converting Enzyme; FAS, Fas cell surface death receptor; HSP, Heat Shock Protein.

Topical application of MSCs can be an effective method to deliver many stem cells to the injured liver.

To compare the therapeutic potential of topical MSCs, an equivalent amount of MSCs was transplanted in all groups. MSCs ( $4 \times 10^6$ ) were administered via the portal vein or tail vein to rats with liver injury. The optimal cell dosage of MSCs transplanted in experimental models remained unclear from the published literature, and the dosage of MSCs used in this study was similar to the description by Song and colleagues.<sup>16</sup>

In this study, the survival of ADMSCs delivered by topical application or portal vein infusion was adversely affected by the hypoxic, nutrient-poor, inflammatory microenvironment of the injured liver. As prolonged exposure to this hostile microenvironment was lethal, no viable GFP+ve ADMSCs were detected in the liver parenchyma 14 days after transplantation. The ischemic liver tissue might release specific homing signals that could attract the ADMSCs to the site of liver injury. Alternatively, in hepatic IRI, there was recruitment of activated neutrophils, which produced toxic enzymes (eg, elastase and serine protease), and reactive oxygen species (eg, superoxide anion, hydrogen peroxide, and hydroxide radicals).<sup>17</sup> We postulated that the migrating ADMSCs might have died or degenerated, leaving behind the iron particles that were detected by Prussian blues staining.

In this study, a comparison between group A (topical MSC application) with group B (portal vein MSC infusion) and group C (tail vein MSC infusion) was not undertaken because there were high mortality rates in the study rats (group B, 50%; group C, 62.5%). This was a consequence of the limited feasibility of MSCs transplantation by portal and tail venous infusions.<sup>18</sup>

Although the histology of scars in group A and group D was similar, the injured liver in the group A developed less necrosis after IRI. In the presence of topically applied ADMSCs, there were smaller necrotic areas and larger regeneration scars. The homed ADMSCs demonstrated spindle-shaped morphology, but did not differentiate to any liver-specific cell type, except for the expression of HNF-4 and HNF-1. There is increasing evidence that suggests the therapeutic effects of MSCs in the liver do not depend on the transdifferentiation into hepatic lineages. The biochemical mechanisms might be through paracrine actions, such as induction of endogenous stem cell (stellate cell) proliferation.<sup>19,20</sup> Topical application of MSCs could offer an additional advantage because

these biofactors could be delivered directly or locally to the injured liver. In this study, the signaling pathways of the topical ADMSCs on the liver surface were significantly activated.

The infusion of ADMSCs into portal circulation caused a high mortality (62.5%) in this study. Additionally, local infusion was technically demanding compared with topical application. The cell suspension must be gently titrated using small needles to keep the ADMSCs dispersed and free of cell clumps. These extra manipulations inevitably damaged cell membranes and reduced the viability and engraftment of the ADMSCs. Topical application might overcome these disadvantages and allow for a more efficient delivery of MSCs to the target organ.

One of the major hurdles to stem cell therapy is the lack of an effective and reproducible transplantation method. Systemic delivery of ex vivo MSCs is feasible but has an obvious drawback, as the homing efficacy of this administration route is low. The uptake of systemically infused MSCs by other somatic organs, for example, the lung might cause potential risks. We have demonstrated significant pulmonary complications with trapped MSCs. Our present study has established the safety of topical application by showing that ADMSCs did not spread to other organs. Moreover, no intravenously injected ADMSCs were detected in the injured liver, demonstrating the low efficiency of systemic administration. We have also shown that topically applied stem cells avoided the potential surgical complications related to portal vein infusion.

Fibrin glue is a useful matrix haemostatic sealant in surgery.<sup>21</sup> It can be used as a keratinocyte carrier to treat skin trauma. Fibrin glue technology has been applied to tissue engineering, for example, bone tissue and nerve regeneration.<sup>22,23</sup> In these studies, MSCs were premixed with fibrin glue in a syringe and then applied to the sites of interest. We are the first research group to demonstrate that, first, fibrin glue facilitates ADMSCs attachment onto the recipient liver surface and second, topical ADMSCs alleviate hepatic IRI. Fibrin glue provided a template for cellular proliferation of ADMSCs. When fibrin glue was not added, most ADMSCs detached from the injured liver surface (group D, data not shown). An additional control group of fibrin glue application (without MSC) to the liver surface was not undertaken because the study hepatic perfusion model did not cause blood loss.

In vitro studies have demonstrated that fibrin glue supports the adhesion, proliferation, migration and differentiation of MSCs.<sup>24,25</sup> Whether the fibrin glue influenced the in vivo or in vitro MSC phenotype was not investigated in this study, but would be an intriguing area for further investigation. Moreover, studies of the signalling pathway of MSCs in IRI were conducted using in vitro models<sup>26</sup> because it was difficult to harvest the infused MSCs from the organs or systemic circulation for detailed analysis.

IRI after liver surgery may lead to posthepatectomy liver failure (PHLF). If present, PHLF is manifest by progressive multisystem organ failure, the need for organ support and can result in mortality. The most effective treatment for PHLF is liver transplantation but graft availability remains limited.<sup>27</sup> In vitro studies have shown that MSC can differentiate into hepatocyte-like cells in the presence of specific cellular growth factors.<sup>28</sup> MSCs have the potential to ameliorate the adverse effects of hepatic IRI, and MSC transplantation via the portal vein is the most effective method in animal studies.<sup>29</sup> However, when this is applied to real patients, there are major drawbacks. These include iatrogenic portal vein injury and significant hemorrhage, hence the investigation into the role of peripheral MSCs infusion. Unfortunately, there are reports of embolization of MSCs into the pulmonary circulation,<sup>8</sup> which precludes this technique for MSC administration. Subsequently, the use of topically applied MSCs, as reported in this study, is an alternative technique for delivering the MSCs to the site of liver injury.

In conclusion, this study represented the first report on in vivo signalling pathways of MSCs in hepatic IRI. The data in this article have demonstrated the safety of the topical ADMSCs application. However, many unknowns remain, and future research areas could include the interaction and reciprocal activation of pathways in the topical MSCs and the recipient liver parenchyma after IRI, the effect of the fibrin glue on the MSCs phenotype, and the mechanisms by which ADMSCs transmigrate through the liver capsule and target the injured liver parenchyma.

## CONCLUSIONS

Topical application of MSCs was associated with the reduction in the inflammatory response to hepatic IRI in a rat model.

## REFERENCES

- Saidi RF, Kenari SK. Liver ischemia/reperfusion injury: an overview. *J Invest Surg.* 2014;27:366–379.
- Klune JR, Tsung A. Molecular biology of liver ischemia/reperfusion injury: established mechanisms and recent advancements. *Surg Clin North Am.* 2010;90:665–677.
- Salem HK, Thiemermann C. Mesenchymal stromal cells: current understanding and clinical status. *Stem Cells.* 2010;28:585–596.
- Abdel Aziz MT, Atta HM, Mahfouz S, et al. Therapeutic potential of bone marrow-derived mesenchymal stem cells on experimental liver fibrosis. *Clin Biochem.* 2007;40:893–899.
- Zhao DC, Lei JX, Chen R, et al. Bone marrow-derived mesenchymal stem cells protect against experimental liver fibrosis in rats. *World J Gastroenterol.* 2005;11:3431–3440.
- Saidi RF, Rajeshkumar B, Shariffabrizi A, et al. Human adipose-derived mesenchymal stem cells attenuate liver ischemia-reperfusion injury and promote liver regeneration. *Surgery.* 2014;156:1225–1231.
- Seki T, Yokoyama Y, Nagasaki H, et al. Adipose tissue-derived mesenchymal stem cell transplantation promotes hepatic regeneration after hepatic ischemia-reperfusion and subsequent hepatectomy in rats. *J Surg Res.* 2012;178:63–70.
- Gao J, Dennis JE, Muzic RF, et al. The dynamic in vivo distribution of bone marrow-derived mesenchymal stem cells after infusion. *Cells Tissues Organs.* 2001;169:12–20.
- Furlani D, Ugurlucan M, Ong L, et al. Is the intravascular administration of mesenchymal stem cells safe? Mesenchymal stem cells and intravital microscopy. *Microvasc Res.* 2009;77:370–376.
- Lam PK, Ng CF, To KF, et al. Topical application of mesenchymal stem cells to somatic organs—a preliminary report. *Transplantation.* 2011;92:e9–e11.
- Lam PK, Lo AW, Wang KK, et al. Transplantation of mesenchymal stem cells to the brain by topical application in an experimental traumatic brain injury model. *J Clin Neurosci.* 2013;20:306–309.
- Cutrin JC, Boveris A, Zingaro B, et al. In situ determination by surface chemiluminescence of temporal relationships between evolving warm ischemia-reperfusion injury in rat liver and phagocyte activation and recruitment. *Hepatology.* 2000;31:622–632.
- Day YJ, Li Y, Rieger JM, et al. A2A adenosine receptors on bone marrow-derived cells protect liver from ischemia-reperfusion injury. *J Immunol.* 2005;174:5040–5046.
- Wang HH, Wang YX, Leung KC, et al. Durable mesenchymal stem cell labelling by using polyhedral superparamagnetic iron oxide nanoparticles. *Chemistry.* 2009;15:12417–12425.
- Akhtar MZ, Henderson T, Sutherland A, et al. Novel approaches to preventing ischemia-reperfusion injury during liver transplantation. *Transplant Proc.* 2013;45:2083–2092.
- Song YM, Lian CH, Wu CS, et al. Effects of bone marrow-derived mesenchymal stem cells transplanted via the portal vein or tail vein on liver injury in rats with liver cirrhosis. *Exp Ther Med.* 2015;9:1292–1298.
- Walsh KB, Toledo AH, Rivera-Chavez FA, et al. Inflammatory mediators of liver ischemia-reperfusion injury. *Exp Clin Transplant.* 2009;7:78–93.
- Xiang J, Tang J, Song C, et al. Mesenchymal stem cells as a gene therapy carrier for treatment of fibrosarcoma. *Cytotherapy.* 2009;11:516–526.
- Jin G, Qiu G, Wu D, et al. Allogeneic bone marrow-derived mesenchymal stem cells attenuate hepatic ischemia-reperfusion injury by suppressing oxidative stress and inhibiting apoptosis in rats. *Int J Mol Med.* 2013;31:1395–1401.
- Baraniak PR, McDevitt TC. Stem cell paracrine actions and tissue regeneration. *Regen Med.* 2010;5:121–143.
- Jackson MR. Fibrin sealants in surgical practice: an overview. *Am J Surg.* 2001;182(Suppl 2):1S–7S.
- Yamada Y, Boo JS, Ozawa R, et al. Bone regeneration following injection of mesenchymal stem cells and fibrin glue with a biodegradable scaffold. *J Craniomaxillofac Surg.* 2003;31:27–33.
- Pan HC, Yang DY, Chiu YT, et al. Enhanced regeneration in injured sciatic nerve by human amniotic mesenchymal stem cell. *J Clin Neurosci.* 2006;13:570–575.
- Bensaid W, Triffitt JT, Blanchat C, et al. A biodegradable fibrin scaffold for mesenchymal stem cell transplantation. *Biomaterials.* 2003;24:2497–2502.
- Park H, Karajanagi S, Wolak K, et al. Three-dimensional hydrogel model using adipose-derived stem cells for vocal fold augmentation. *Tissue Eng Part A.* 2010;16:535–543.
- Pan GZ, Yang Y, Zhang J, et al. Bone marrow mesenchymal stem cells ameliorate hepatic ischemia/reperfusion injuries via inactivation of the MEK/ERK signaling pathway in rats. *J Surg Res.* 2012;178:935–948.
- Manns MP. Liver cirrhosis, transplantation and organ shortage. *Dtsch Arztebl Int.* 2013;110:83–84.
- Wang PP, Wang JH, Yan ZP, et al. Expression of hepatocyte-like phenotypes in bone marrow stromal cells after HGF induction. *Biochem Biophys Res Commun.* 2004;320:712–716.
- Sun L, Fan X, Zhang L, et al. Bone mesenchymal stem cell transplantation via four routes for the treatment of acute liver failure in rats. *Int J Mol Med.* 2014;34:987–996.